Book of Tutorials and Abstracts

European Microbeam Analysis Society

EMAS 2025

18th

EUROPEAN WORKSHOP

on

MODERN DEVELOPMENTS AND APPLICATIONS IN MICROBEAM ANALYSIS

11 to 15 May 2025
at the
TecnoCampus
Mataró (Barcelona), Spain

Organized in collaboration with the
Universitat de Barcelona, Spain

EMAS
European Microbeam Analysis Society eV
www.microbeamanalysis.eu/

This volume is published by:
European Microbeam Analysis Society eV (EMAS)
EMAS Secretariat
c/o Eidgenössische Technische Hochschule, Institut für Geochemie und Petrologie
Clausiusstrasse 25
8092 Zürich
Switzerland

ISBN 978 90 8227 6985
NUR code: 972 – Materials Science

COMBINED EDS AND WDS QUANTITATIVE ANALYSES: THE BEST OF BOTH WORLDS

Julien M. Allaz[1], L. Martin[1,2], J.-C. Storck[1], P. Ulmer[1], E. Reusser[1], R.-G. Popa[1], A. Chatterjee[1] and O. Bachmann[1]

1 ETH Zürich, Department of Earth and Planetary Sciences
Clausiusstrasse 25, 8092 Zürich, Switzerland
2 Current address: NAGRA
Hardstrasse 73, Postfach, 5430 Wettingen, Switzerland
e-mail: julien.allaz@eaps.ethz.ch

Julien M. Allaz was born in the French part of Switzerland. He obtained an MSc (2003), and a PhD (2008) in Geology at the Universities of Lausanne and Bern (Switzerland), respectively. During his early career, he focussed on structural geology and metamorphic petrology in the Central Alps of Switzerland, which required a large dose of electron microprobe analysis (Cameca SX-50, then JEOL JXA-8200), isotopic work, and extended fieldwork. His attraction to the microprobe and scanning electron microscope led him to a post-doc at the University of Massachusetts-Amherst on trace element analyses and monazite dating by EPMA from 2009 (Cameca SX-50 + SX 100). In 2012, he became a Research Associate at the University of Colorado Boulder and managed the electron microprobe laboratory (JEOL JXA-8600, then -8230). In 2018, he took a position as head assistant for the electron microprobe (JEOL JXA-8200, then -8230) and the scanning electron microscopy laboratories (JEOLJSM-6390) at the Institute of Geochemistry and Petrology at the Swiss Federal Institute of Technology in Zurich (ETH Zürich, Switzerland), and in 2020, he became the lab manager of those labs. Julien also has a strong attraction to websites and coding, and has notably created a "database of electron microprobe analysis" (https://de-ma.ch/) and a focussed interest group on microanalytical standards (https://figmas.org; founded in 2016 with A. von der Handt and O.K. Neill). His current research interests include magmatic petrology, geochronology, ore deposits notably REE, and the development of new analytical setup for electron microprobe work notably on beam sensitive materials.

1. ABSTRACT

This paper focuses on the ability of an electron probe microanalyser (EPMA) or a scanning electron microscope (SEM) equipped with wavelength- and energy-dispersive X-ray spectrometers (WDS and EDS) to use both these detectors for their standard-based quantitative X-ray analysis to yield precise and accurate compositions. This approach can be extremely useful to improve the analytical capabilities at the micron-scale, notably to:

(a) Reduce the total analysis time,
(b) Improve the precision and accuracy on minor and trace elements in beam sensitive materials,
(c) Improve the accuracy by choosing WDS analysis for elements suffering from a poor peak-to-background ratio and low count rate on EDS (e.g., trace elements, light elements) or of a strong interference by EDS,
(d) Permit the post-analysis quantification of an unsuspected element,
(e) Enable a lifeline to salvage quantitative data after a WDS hardware failure or a change in the environment affecting one or more WDS (i.e., room temperature),
(f) Or a combination of the above, and possibly more.

First, we evaluate the reliability of EDS versus WDS data in geological samples on our EPMA and SEM instruments. A general silicate analysis setup is designed to prove that identical results can be obtained for major and minor elements down to ~ 0.5 wt% in a variety of common rock-forming minerals. Next, two real-case applications of combined EDS-WDS analysis are presented: (1) Halogens and few minor to trace elements analysis in apatite, such as S, Ce, Si, Na, Fe, Mg, and Mn at low current and high resolution (≤ 10 nA, 2 to 10 µm beam size) and Ca and P analysed by EDS, and (2) Trace analysis of P-in-olivine (and other elements such as Cr and Al) at high current (≥ 200 nA) and focussed beam with Si, Fe, Mg, and Mn by EDS.

2. INTRODUCTION

The core principle of any chemical microanalyses on electron microscopes is to count over a certain time the number of characteristic X-rays generated by a focussed beam of electrons that has a certain initial energy (acceleration voltage) and density (beam current). Nowadays, two major device types are used for counting X-rays: Energy- and wavelength-dispersive X-ray spectrometers (EDS and WDS). The first measures the energy of each incoming X-ray, whereas the latter filters out X-rays based on their wavelength. In both cases, results are usually reported at a certain acceleration voltage as a net intensity (corrected for the bremsstrahlung) normalised to the analysis time and electron beam current (i.e., counts per second per nanoampere or cps/nA). A first step to render this characteristic X-ray intensity quantitative, is to compare it with a reference value, either constrained by some factory-based factors or reference spectra for each element ("standardless" approach) or using a set of reference materials or "standards" data acquired in the lab prior to the analysis ("standard-based" approach).

The "standardless" approach usually relies on factory-defined calibration factors obtained on a reference detector and some reference material acquired on this detector. The most ambitious approach is the "first principles standardless", which uses only physical calculations of the X-ray generation, propagation, and detection based on the instrument and detector geometry [1]. A more common approach is the "remote standards", which relies on a library of spectra acquired in reference materials at several beam energies on a known EDS detector. This library is then used to estimate the intensities of the same element in a different environment with possibly different beam energies, take-off angle, and detector efficiency (Newbury, 2012; pers. comm.). Those factors are used along with a correction for the electron microscope and EDS geometry. The X-ray counts are then quantified and normalised to 100 wt%. Theoretically, the user does not need a reference material to quantify the data, although some software may propose an adjustment factor based on the measurement of one or more reference materials.

The "standard-based" approach requires the measurement be on a specific instrument at the same acceleration voltage of a characteristic X-ray intensity, both in a standard or reference material of known composition and in the unknown. It is highly reliable, yet it requires the presence of standard materials. By comparing the ratio of both net intensities normalised to the analysis time and beam current, we obtain a so-called "k-ratio":

$$k_{ratio} = I_{unknown}^{X-ray\ element\ A} \Big/ I_{standard}^{X-ray\ element\ A}. \quad (1)$$

This *k*-ratio multiplied by the wt% element *A* in the standard is a first approximation of the wt% concentration of element *A* in the unknown, a formula known as Castaing's first approximation [2]:

$$C_{unknown}^{element\ A\ [wt\%]} \approx C_{standard}^{element\ A\ [wt\%]} \cdot k_{ratio}. \quad (2)$$

Whether we consider the "standardless" or "standard-based" approach, a matrix correction must be applied to compensate for the difference in nature between the unknown analysed material and the standard used either in standardless or the standard-based approach. Such a method is commonly referred to as the ZAF correction:

- Z-factor: Materials of different density and atomic number Z will show different stopping power and backscattering coefficients.
- and F-factor: the generated X-ray inside the material can potentially be absorbed (A: absorption) and has a certain potential to ionize another element and generate a secondary characteristic X-ray (F: fluorescence).

This matrix correction has different flavours that won't be reviewed here (e.g., PROZA, PAP, CITZAF [3-5]). For this paper, we will exclusively rely on an adaptation of the matrix correction of [4] on all systems considered here, and the choice of this matrix correction does not affect the main conclusions.

X-ray microanalysts in need of precise and accurate quantitative data at the micrometre-scale have been relying almost exclusively on data from electron probe microanalyser (EPMA) and its WDS for 70+ years [2]. With its high wavelength (energy) resolution, WDS has been the norm to discriminate X-rays, to minimise X-ray interferences (or properly correct for them using standards), and to provide analysts with accurate data. This is of course correct at the condition that a) the *k*-ratio approach is used with appropriate standards to compare each characteristic X-ray intensity, with a daily to weekly standardisation, and b) a matrix correction is properly applied.

Quantitative analysis by EDS has long been rejected by many reviewers especially in the geological sciences community, qualifying them as "inaccurate" data, sometimes with good justification, or sometimes just because EDS is not trusted to generate good quantitative data. This contribution hopes to change the misbelief that EDS data cannot be precise and accurate, and, more importantly, to explain how to ensure good precision and accuracy. By taking advantage of both worlds with EDS for major elements analysis (± minor) and WDS for minor and trace elements, more efficient and precise analyses can be defined for the betterment of microanalytical science.

3. PRECISE AND ACCURATE EDS AND WDS ANALYSIS

3.1. SEM and EDS

EDS has been used for 55+ years, with the first Si(Li)-detectors having been developed in the late sixties [6]. Recent improvements in past decades in both hardware and software allow faster and more efficient X-ray collection, notably with the development of silicon drift detectors (SDD) [7, 8], electronic improvements for faster counting and processing, and novel detector geometries (see review in [9]). Standardless analysis commonly yields inaccurate and rarely trustable data at the level we require (i.e., 1 - 2 % accuracy, ~ 0.5 % precision uncertainty for major and minor elements), especially when light elements are missing in the analysis and not specified during the quantification (e.g., H, Li, B, C). Reported relative standard deviation from accurate values are on the order of ± 50 % for standardless analysis on old Si(Li)-detectors and around ± 5 - 10 % for the newest SDD EDS detectors [1, 9]. Newbury and Ritchie [10] demonstrated that precise and accurate results of major (> 10 wt%) and minor elements (1 - 10 wt%) can be obtained by EDS with either a Si(Li)-detector or an SDD providing that a standard-based approach and a proper matrix correction such as ZAF or φ(ρz) is considered. Even elements in the 1.0 to 0.1 wt% range can be analysed if enough counts are collected [11-13]. Limitation of EDS analysis of major and minor elements (> 1 wt%) arises when it comes to spectral resolution and X-ray interferences. It is however possible to obtain decent results down to ~ 1 wt% in the presence of strong interferences such as lanthanides L-lines, if poor precision and accuracy is tolerated. For this, a careful peak shaping should always be done in

an interference-free reference material (e.g., Ce-L lines on synthetic $CePO_4$ instead of a natural monazite; [14]). Resulting analyses will still suffer from large accuracy uncertainties in the range of 5 to 10 % despite minutes-long acquisition on (multiple) large area SDD [13, 15].

3.2. EPMA and WDS

EPMA with its multiple WDS is still considered to be the prime instrument for precise and accurate quantification of elements of atomic number $Z > 9$ (F), and numerous books and reviews are available [16-18]. Even light elements ($Z = 4$ to 8; Be to O) can be analysed [3], with difficulties that will not be addressed in this paper. WDS is still considered to be the norm for microanalysis of major and minor elements at high X-ray spectral resolution and high spatial resolution. The main advantage of WDS is its ability to filter X-rays: Only a selected wavelength (λ) of a certain order (n) can be diffracted at a defined diffraction angle (θ) on a monochromator of known lattice spacing (d) according to the Bragg's law of diffraction:

$$n \cdot \lambda = 2d \cdot \sin\theta\,. \tag{3}$$

This filtering of X-rays results in a better peak-to-background ratio compared to EDS ("background" meaning here the bremsstrahlung X-ray signal), which translates into higher sensitivity and lower detection limits. The better spectral resolution compared to EDS, especially at high $\sin\theta$-value (= high spectral resolution on WDS), also helps to prevent element misidentification and minimises spectral interferences. Several X-ray monochromators are available with 2d lattice spacing varying from 1.801 (LiF420) to ~ 200 Å with synthetic pseudo-crystals (e.g., PC3 or LDE3) to cover all X-ray energies from ~ 0.1 up to ~ 25,000 eV. Some improvements were made in past decades to improve the collection efficiency, notably with smaller Rowland circle spectrometers (e.g., H-type at 100 mm and "normal" at 140 mm [JEOL] or 160 mm [Cameca]), and with the availability of large-area monochromators (L-type) that offer higher count rates at excellent spectral resolution (see a comparison in [15]).

SEM-EDS manufacturers also propose WDS detectors mounted on an SEM (e.g., Bruker XSense, EDAX Lambda, Oxford Inca Wave, Thermo Fisher Scientific MagnaRay). Such devices typically use either a large Rowland circle (e.g., 210 mm) like a WDS on EPMA or more commonly a focussing polycapillary optics system. The latter produces a parallel beam of X-rays that is then diffracted by a monochromator and sent to a scintillator for high X-ray energy lines or to a P_{10} gas flow proportional counter (90 % Ar + 10 % CH_4) for low X-ray energy lines. The polycapillary optics system provides a higher count rate compared to a Rowland circle and can be as good as EPMA-WDS, if not better [19, 20]. Spectral resolution is the best when considering Rowland circle focussing, the polycapillary optics system lowers the spectral resolution, but is still significantly better than EDS ([20] and M. Abratis [Bruker], pers. comm., 2025). The authors do not have access to such a device, and, therefore, it will not be evaluated in this paper. Nevertheless, it should be emphasised that the following discussion on combined EDS-WDS analysis should also apply to SEMs equipped with both an EDS and a WDS.

4. *INSTRUMENTS AND METHODS*

Most data presented in this paper were acquired at the Department of Earth and Planetary Sciences at ETH Zürich (Switzerland) on a JEOL JXA-8230 EPMA. A few extra data were obtained by the first author at the University of Colorado, Boulder (USA) on a similar JXA-8230 EPMA. Although not shown in this manuscript, a JEOL JSM-6390LA SEM equipped with a 30 mm^2 Thermo Scientific UltraDry EDS (129 eV resolution at Mn-Kα) was also used and ultimately provided similar standard-based quantitative analyses, notably in beam sensitive glasses. These data will be presented in the published version of this Workshop manuscript and briefly shown during this workshop. All instruments are equipped with an in-column Faraday cup to measure the beam current. All investigated standards and samples were polished and coated with 20 nm carbon using a fully refurbished Edwards E306 carbon evaporator.

The JEOL JXA-8230 EPMA at ETH Zürich is equipped with 5 WDS and a 30 mm^2 JEOL SDD EDS detector (129 eV resolution at Mn-Kα). All data were processed using the PROBE FOR EPMA software from Probe Software. EDS deadtime was around 30 - 40 % for acquisitions at 20 nA and around 15 - 30 % for acquisition at 10 nA. For high-current application (> 50 nA), the EDS detector window was reduced and sometimes a shorter time constant was used (T3 = 1.6 µs) to accommodate the high count-rate and to ensure < 50 % deadtime. WDS acquisition time and monochromator selection varied depending on the analysed material, and detailed analytical setups are described in the following.

A JEOL JXA-8230 EPMA at the University of Colorado, Boulder (USA) was also used for some examples listed below. This EPMA is equipped with a 10 mm^2 UltraDry SDD detector with 129 eV resolution at Mn-Kα. Data were processed through the PATHFINDER software of Thermo Fisher Scientific.

4. *COMPARING EDS AND WDS RESOLUTION*

WDS enables a much higher peak-to-background ratio and an order of magnitude better spectral resolution than EDS. For instance, a spectral resolution of ~ 10 to 40 eV is achieved on LiF200 monochromator for energies of 4.6 to 8.5 keV [15] to compare with 121 eV at best for Mn-Kα at 5.9 keV (Fano limit). At lower energies (~ 0.5 to 2 keV), PET and TAP monochromators yield a resolution of ~ 2 to 10 eV compared to ~ 50 to 75 eV on recent SDD EDS detector (e.g., Si-Kα; Fig. 1). Higher energy resolution and peak-to-background ratios translate into higher analytical sensitivity, lower detection limits, and higher precision for elements below 1 wt%. L-type monochromators significantly improve the collection efficiency and thus provide a higher count rate at a similar spectral resolution, and H-type spectrometers with a smaller Rowland circle also provide a higher count rate, but at the cost of a slightly lower spectral resolution [15]. EPMA equipped with up to 5 WDS with L-type monochromators or H-type spectrometers can, therefore, routinely reach detection limits in the 10- to 100-ppm range for

element Z ≥ 11 (Na). Detection limits as low as 1 to 10 ppm can be reached under certain conditions providing a high beam current and a long counting time are considered to reach the desired counting statistics [21-26].

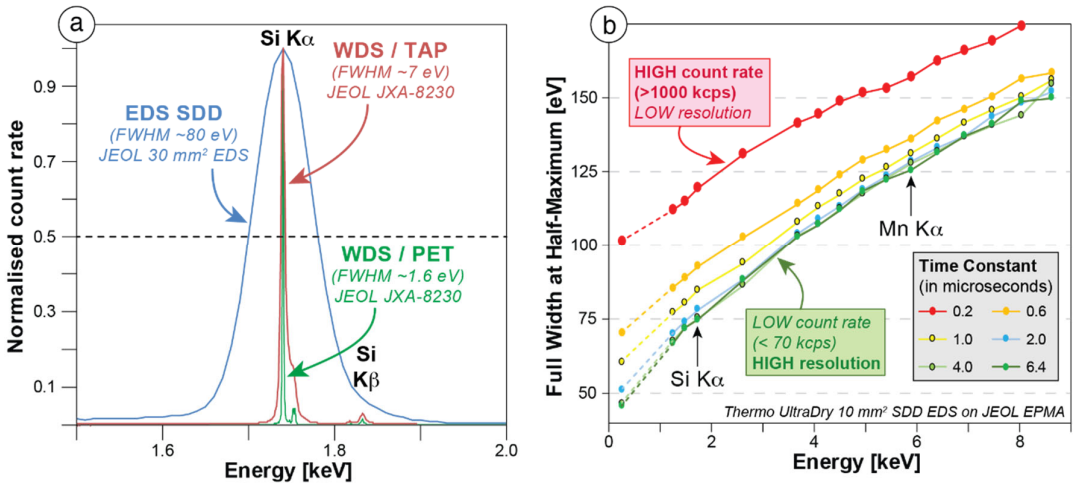

Figure 1. a) Comparison of Si K-lines by EDS and WDS in quartz (SiO_2). Data from JEOL JXA-8230 EPMA using TAP and PET monochromators and JEOL JSM-6390 SEM using a JEOL 30 mm^2 SDD EDS at time constant T4 (3.2 µs) and ~ 35 % deadtime. FWHM for Si is ~ 80 eV for SDD EDS, ~ 7 eV for TAP and ~ 1.6 eV for PET monochromator on WDS. b) Evaluation of full width at half maximum in pure element standards using a 10 mm^2 Thermo UltraDry SDD EDS at the University of Colorado, Boulder, at various time constants and 20 to 30 % deadtime.

5. *EDS DEADTIME CORRECTION*

EDS detector requires the user to define a time-constant for the processing of an incoming X-ray, which will affect the energy resolution and deadtime percentage. This paper will not discuss how such a correction is applied; we rely entirely on the hardware and software used. However, we performed tests based on our analytical needs. For instance, major and minor element analysis in common geological samples and silicate rocks requires precise measurement of Si and Al, for example in plagioclase, pyroxene, or amphibole minerals. To guarantee a good measurement, a crucial point is to fully discriminate Si-K and Al-K X-ray lines, which are separated by only ~ 250 eV. This is achievable on all the EDS systems considered here when the time constant is set to > 1 µs and is even better at ≥ 3 µs.

Accurate analysis requires careful consideration of the EDS deadtime percentage (DT%), which is the percentage of real time the system is processing an X-ray count and is unable to assess the energy level of any other incoming X-ray. Manufacturers have their own recommendations for efficient analyses, usually between 20 and 40 DT%. With higher DT% comes more EDS

artefacts, especially sum peaks. This artefact occurs when two X-rays hit the detector simultaneously and are processed as a single event at an energy level corresponding to the sum of the two (or more) X-rays. EDS software is usually equipped with a statistical tool to remove sum peaks and to add them back to their effective X-ray peaks (compare Figs. 2a and 2b and Figs. 2c and 2d). Despite good efforts, traces of sum-peaks might remain above 50 DT%, and are largely unnoticed below 30 DT% for the considered acquisition time and beam conditions (Figs. 2a and 2b). The problem tends to be stronger in the optimum energy range of the EDS detector considered (~ 1.2 keV for the considered EDS SDD), as the count rate on each individual energy channel is higher. If too many sum-peaks remain unaccounted for, the risk for quantitative analysis is to either lower the actual count rate of the concerned elements (e.g., less Si-K counts for uncorrected Si+O, Si+Mg, Si+Si sum peaks) or to abnormal increase the count rate when the sum peaks interfere (e.g., higher counts on Si-K due to Mg+O sum peak; Fig. 2a).

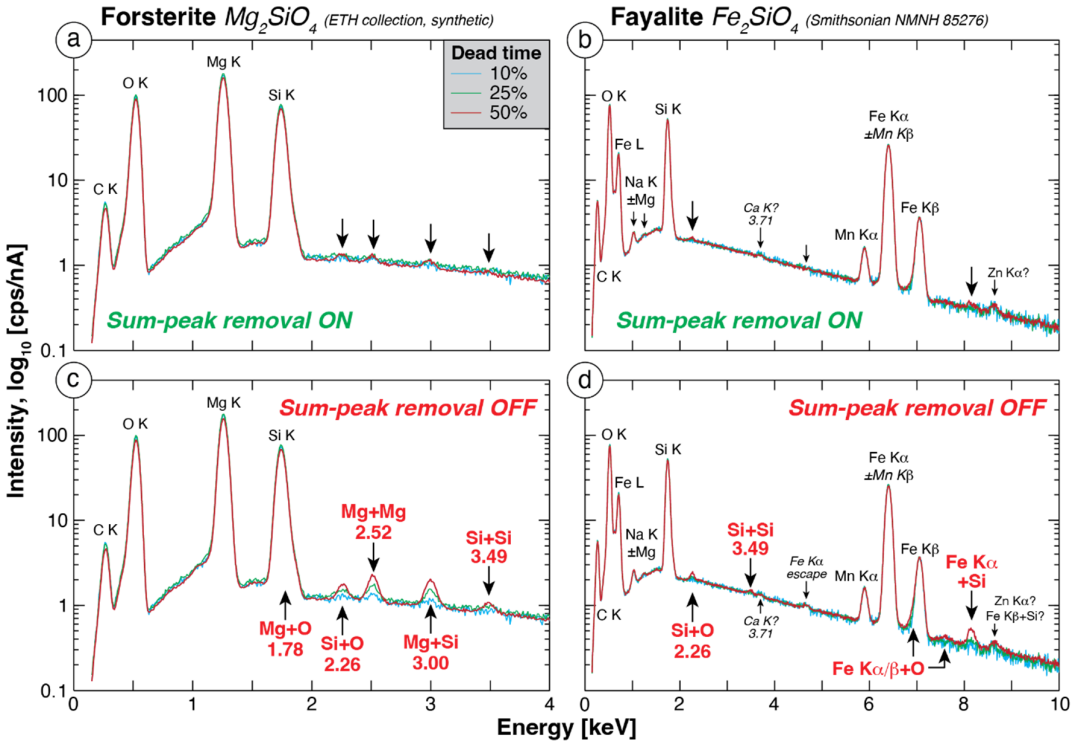

Figure 2. Results of 60 s EDS analyses in (a and c) synthetic forsterite (Mg_2SiO_4) or (b and d) natural fayalite NMNH 85276 (Fe_2SiO_4; right) from the Smithsonian Institute at 10, 25 and 50 DT% on JEOL SDD EDS. (a and b) show EDS after sum-peak removal from JEOL software, and (c and d) show the same EDS data without sum-peak removal. Values below identified sum peaks correspond to energy level. Unlabelled arrows in (a and b) point to major sum peak positions.

6. *ACCURACY OF EDS VERSUS WDS DATA*

Evaluation of EDS and WDS accuracy is done by considering silicate analysis in geological materials of known composition (i.e., secondary standards). A general setup commonly used at ETH on the JEOL JXA-8230 EPMA aims to measure a large variety of rock-forming silicates and oxides with the analysis of Si^{4+}, Ti^{4+}, Cr^{3+}, Al^{3+}, Fe^{2+} (or Fe^{3+}), Mn^{2+}, Mg^{2+}, Ca^{2+}, Na^{+}, and K^{+} (all Kα-lines for WDS and Kα+Kβ for EDS) at 15 keV, 20 nA beam current, variable beam size, and with oxygen calculated by stoichiometry to the assumed cation valence (Table 1). This setup is sometime complemented by analysis of P^{5+} and Ni^{2+} (not shown here). Similar setups are used in many geological laboratories to analyse (for example) olivine, pyroxene, feldspar, amphibole, mica, garnet, and some oxides.

Table 1 Analytical setup on the JEOL JXA-8230 at ETH Zürich for general silicate analyses by WDS or EDS. For analyses where precision should be better for Ca or Cr, those elements are placed on spectrometer 3 (large area PET-L monochromator), and K and Ti are moved to spectrometer 2 (normal PET-J monochromator). All WDS on-peak X-ray counts are corrected for the Bremsstrahlung using the mean atomic number background correction [27]. The energy range considered for EDS data is also given for the K-line X-ray family.

Acc. voltage	15 keV
Beam current	20 nA
Beam size	10 µm (standard), 0 to 5 µm (unknown)
EDS	30 s live time, T4 time constant (3.2 µs), open window

El.	Xtal	SP	EDS energy [keV]		Standard
Si Kα	TAP	1	1.60	2.01	Piz Beverin albite
Al Kα	TAP	1	1.34	1.64	Anorthite (U. Wien)
Ca Kα	PETJ	2	3.52	4.18	Anorthite (U. Wien)
Cr Kα	PETJ	2	5.22	6.12	Chromite, Stillwater (OR, USA)
K Kα	PETL	3	3.10	3.80	Sanidine (Madagascar)
Ti Kα	PETL	3	4.27	5.12	Rutile (synthetic)
P Kα	*PETL*	*3*	*1.88*	*2.26*	*Wilberforce apatite*
Fe Kα	LiFH	4	6.18	7.28	Fayalite (NMNH 85276)
Mn Kα	LiFH	4	5.68	6.70	Pyrolusite MnO2
Ni Kα	*LiFH*	*4*	*7.21*	*8.49*	*Bunsenite NiO*
Na Kα	PETH	5	0.91	1.19	Piz Beverin albite
Mg Kα	PETH	5	1.06	1.43	Forsterite (synthetic)

Data accuracy strongly depends on the calculation of the *k*-ratio and the stability of the reference element intensity measured on a standard. Therefore, we first evaluate the stability of each system. A comparison of 8 individual standardisation sessions by WDS and EDS obtained over 3 months (December 2024 to March 2025) is summarised in Fig. 3 by checking the ratio of the average count rate for one element in one session normalised to the average of all count rates for that element throughout all sessions. Data are acquired on WDS for 30 s on the X-ray peak position of each element of interest (or 20 s if three elements are stacked on one WDS), and EDS is acquired simultaneously for 30 s at 30 to 40 DT% (3.2 µs time constant). Reference materials

are first analysed at 20 nA and 10 µm beam size. Bremsstrahlung correction of WDS data is done using the mean atomic number (MAN) background correction [27] through PROBE FOR EPMA.

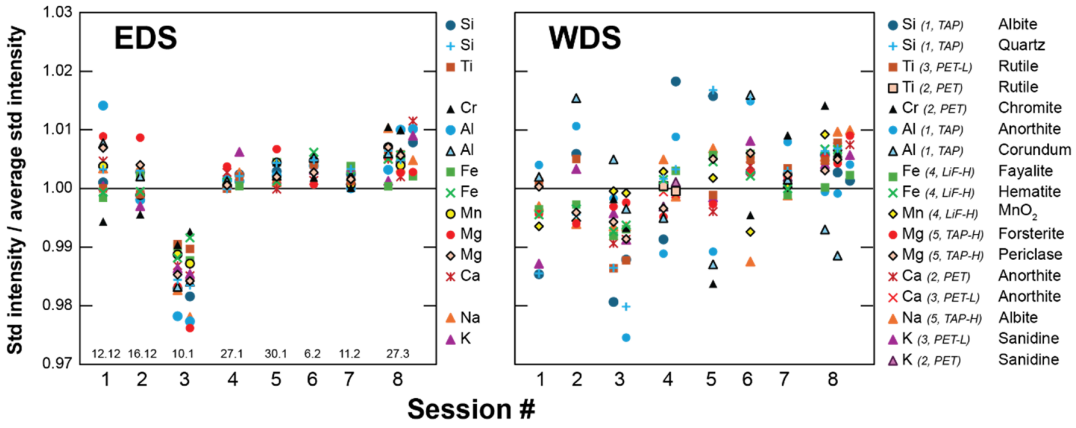

Figure 3. Comparison of normalised X-ray intensities of major elements in silicate and oxide standards obtained simultaneously by EDS and WDS. Each point is an average of 4 to 8 individual measurements. Uncertainty of each measurement is better than 0.5 % relative (1σ) and commonly below 0.3 %. Each datum is normalised to the overall average of all measurements over the 3-month period.

Repetition of standard analyses over a 3-month period highlights the high stability of EDS systems. Except for session #3, all EDS data remain ± 0.5 % from the overall average (Fig. 3). It is unclear why session #3 yielded ~ 1 % lower intensities, although it was done only a couple hours after an annual maintenance with several ventings and power-downs of the instrument, and possibly the vacuum was not "good enough" (low 10^{-3} Pa range) or the SDD detector was not in a steady-state cooling stage. On the contrary, WDS and pulse height analyser detectors, especially P_{10} gas flow proportional counters, are sensitive to changes in the environment (room temperature, dew point and atmospheric pressure for the gas flow proportional counter, etc.; [28]) and to the precision in the mechanical reproducibility of the spectrometer motor. Stability is usually guaranteed within ± 1 % or better for a single session occurring over 2 – 3 days or more providing there is no change of monochromator or of the environment conditions (e.g., sessions 3 and 4 with two and three full standardisations in Fig. 3). There are few exceptions, notably for Si-Kα and Al-Kα calibration, where the X-ray peak on the TAP monochromator is very narrow, and an extremely good spectral resolution is available (full width at half maximum at ~ 5 to 10 eV; Fig. 1a). A regular standardisation for WDS is, therefore, recommended every few days, whereas EDS standardisation seems to hold well within ± 0.5 % variation once everything is stabilised.

To check for data accuracy and possible session-to-session stability, the analysis of secondary reference materials is necessary. We consider the collection of microbeam reference materials from the Smithsonian Institute [29, 30] and the following minerals: Kakanui (NMNH 143965) and Arenal hornblende (NMNH 111356), Lake County plagioclase (NMNH 115900), and San Carlos (USNM 2566) and Springwater olivine (NMNH 111312-44). All data were obtained in different sessions over a period of 3 years, and results are given as averages in Table 2.

Concentration of each secondary standard is obtained by considering the measurements only by WDS or only by EDS. For comparison of different software, data are processed either with the JEOL PC-EPMA software or with PROBE FOR EPMA. When JEOL PC-EPMA software is used, a two-point background acquisition is performed on each point at an interference-free spectrometer position. For PROBE FOR EPMA, the MAN background correction is considered. For each software, the mathematical treatment of the characteristic X-ray intensities (i.e., net intensity as cps/nA) is the same for WDS-only or EDS-only data: Net intensities are corrected for deadtime and bremsstrahlung, *k*-ratios are calculated (eq. 1), a first composition is calculated using Castaing's first approximation (eq. 2), and the data are sent through the matrix correction. EDS data are extracted from the spectrum using a region of interest set by the JEOL software for each element and are then sent to PC-EPMA or to PROBE FOR EPMA for quantification.

There is excellent agreement between EDS and WDS for all major and minor elements > 1 wt% measured in common geological materials, independent of the software used. Data acquired simultaneously on the same spot at the same time (e.g., data from 8.9.2021) yield very close results. Kakanui hornblende yield 40.73 ± 0.18 versus 40.66 ± 0.18 wt% SiO_2 and 2.58 ± 0.06 versus 2.60 ± 0.07 wt% Na_2O for EDS versus. WDS. The only clear distinction is for elements below 0.5 wt%, with significantly higher standard deviation (Table 2). EDS yields accurate results for minor elements, yet only after several repetitions and, therefore, long counting times (> 2 - 3 minutes). For instance, 76 individual measurements obtained in Kakanui hornblende on 8.9.2021 show a variation for MnO wt% from 0 to 0.225 % by EDS, whereas the WDS measurement varies only from 0.072 to 0.110 %, yet both data yield similar averages at 0.10 ± 0.07 by EDS and 0.090 ± 0.009 wt% MnO by WDS (reference value = 0.09 wt%). The same applies to K_2O analysis in Lake County plagioclase, with 17 EDS data varying from 0 to 0.15 wt% and 20 WDS data varying only between 0.112 to 0.145 wt%. Although the averages are lower than the reference value (0.18 wt%), the values acquired by EDS or WDS are in line with data form [32] (0.116 ± 0.011 wt% K_2O, individual values from 0.090 to 0.140). For elements below 100 ppm such as Cr_2O_3, WDS analysis returns an average of 0.006 ± 0.005 (single point from -0.005 to 0.017), whereas EDS is 0.06 ± 0.06 (single point from 0 to 0.24). Both are insignificant and close or below detectability calculated at 0.06 for EDS and 0.009 wt% for WDS, yet the EDS data tend to commonly return "false positives" with abnormally high values that appear to be above the calculated detection limit. The reason is due to the poor peak-to-background ratio and the inability of the software to return negative values: It returns zero if the calculated bremsstrahlung intensity is higher than the element intensity. By doing so, the average tends to be higher and may lead the analyst to believe that this element "could" be

Table 2. Standard-based analysis on five secondary standards from the Smithsonian Institute [30]. Data acquired using either the EDS (blue-shaded cells) or WDS (green-shaded) detector and processed through JEOL PC-EPMA or PROBE FOR EPMA (PfE) software. Average and standard deviation (1σ) based on several points indicated under "# points". Data in red are below detection limit. Reference composition according to [30] (Ref. A) or [31] (Ref. B). n.d. = not determined. H_2O content of amphibole calculated by stoichiometry.

		Kakanui hornblende						Arenal hornblende				
	Detector			EDS	**EDS**	**WDS**	WDS			**EDS**	**WDS**	WDS
	Software			PfE	**PfE**	**PfE**	JEOL			**PfE**	**PfE**	JEOL
	Acq. date			4.1.22	**8.9.21**	**8.9.21**	27.5.19			**8.9.21**	**8.9.21**	27.5.19
	# points	*Ref. A*	*Ref. B*	5	**76**	**76**	20	*Ref. A*	*Ref. B*	**93**	**93**	20
Averages	SiO_2	*40.37*	*40.40*	40.64	40.73	40.66	40.87	*41.46*	*42.00*	41.97	42.02	42.15
	Al_2O_3	*14.90*	*14.30*	14.01	14.41	14.36	14.59	*15.47*	*14.10*	14.28	14.21	14.53
	TiO_2	*4.72*	*4.96*	4.77	4.79	4.81	4.86	*1.41*	*1.41*	1.33	1.34	1.37
	Cr_2O_3	-	-	0.07	0.06	0.006	0.008	-	-	0.07	0.012	0.007
	FeO	*10.92*	*10.80*	10.54	10.52	10.46	10.52	*11.47*	*11.70*	11.19	11.14	11.24
	MnO	*0.09*	*0.09*	0.12	0.10	0.090	0.086	*0.15*	*0.15*	0.14	0.15	0.15
	MgO	*12.80*	*12.50*	12.56	12.61	12.55	12.61	*14.24*	*14.60*	14.46	14.39	14.47
	CaO	*10.30*	*10.30*	10.12	10.12	10.07	10.07	*11.55*	*11.60*	11.32	11.39	11.33
	Na_2O	*2.60*	*2.71*	2.66	2.58	2.603	2.565	*1.92*	*2.25*	2.13	2.16	2.08
	K_2O	*2.05*	*2.12*	2.11	2.10	2.131	2.159	*0.21*	*0.21*	0.18	0.20	0.20
	NiO	-	-	0.01			0.012	-	-	-	-	0.008
	H_2O	-	-	2.05	2.04	2.04	2.05	-	-	2.05	2.06	2.05
	TOTAL	***98.75***	***98.18***	**99.66**	**100.06**	**99.78**	**100.40**	***97.88***	***98.02***	**99.12**	**99.07**	**99.60**
Standard deviation (1σ)	SiO_2			0.09	0.18	0.18	0.16			0.26	0.24	0.20
	Al_2O_3			0.05	0.09	0.07	0.09			0.21	0.21	0.17
	TiO_2			0.06	0.08	0.05	0.03			0.09	0.06	0.05
	Cr_2O_3			0.08	0.06	0.005	0.012			0.08	0.005	0.010
	FeO			0.14	0.15	0.12	0.10			0.14	0.11	0.12
	MnO			0.08	0.07	0.009	0.014			0.09	0.01	0.01
	MgO			0.05	0.14	0.12	0.09			0.14	0.12	0.10
	CaO			0.09	0.07	0.07	0.06			0.09	0.10	0.08
	Na_2O			0.03	0.06	0.066	0.032			0.11	0.13	0.03
	K_2O			0.03	0.04	0.018	0.017			0.04	0.02	0.01
	NiO			0.02	-	-	0.013			-	-	0.013

		Springwater olivine				San Carlos olivine				Lake County plagioclase			
	Detector		EDS	EDS	WDS		EDS	EDS	WDS		EDS	EDS	WDS
	Software		JEOL	PfE	PfE		JEOL	PfE	PfE		JEOL	PfE	JEOL
	Acq. date		14.6.19	4.1.22	20.10.21		14.6.19	4.1.22	20.10.21		14.6.19	4.1.22	27.5.19
	# points	*Ref. A*	12	3	15	*Ref. A*	12	3	72	*Ref. A*	12	5	20
Averages	SiO_2	*38.95*	39.97	39.81	39.64	*40.81*	41.15	41.06	40.82	*51.25*	52.23	51.68	52.19
	Al_2O_3	-	*n.d.*	*n.d.*	-0.001	-	0.11	*n.d.*	0.027	*30.91*	30.89	30.10	31.08
	TiO_2	-	0.02	0.06	-	-	0.02	*n.d.*	-	*0.05*	0.08	0.04	0.040
	Cr_2O_3	*0.02*	0.03	0.02	0.015	-	0.01	0.07	0.017	-	0.12	0.06	0.003
	FeO	*16.62*	16.84	16.91	16.68	*9.55*	9.72	9.51	9.50	*0.46*	0.41	0.39	0.423
	MnO	*0.30*	0.32	0.29	0.31	*0.14*	0.15	0.14	0.143	*0.01*	0.00	0.03	0.006
	MgO	*43.58*	43.65	43.23	43.09	*49.42*	49.17	48.78	48.70	*0.14*	0.14	0.07	0.132
	CaO	-	0.02	*n.d.*	0.005	*< 0.05*	0.11	0.08	0.096	*13.64*	13.48	13.55	13.32
	Na_2O	-	0.10	*n.d.*	-	-	0.12	*n.d.*	-	*3.45*	3.82	3.84	3.77
	K_2O	-	0.005	*n.d.*	-	-	0.004	*n.d.*	-	*0.18*	0.04	0.11	0.124
	NiO	-	*n.d.*	*n.d.*	-0.002	*0.37*	-	0.36	0.345	-	*n.d.*	0.08	0.011
	H_2O	-	-	-	-	-	-	-	-	-	-	-	-
	TOTAL	***99.47***	**101.03**	**100.31**	**99.75**	***100.29***	**100.56**	**99.99**	**99.65**	***100.09***	**101.21**	**99.97**	**101.10**
Standard deviation (1σ)	SiO_2		0.14	0.07	0.09		0.16	0.09	0.18		0.37	0.05	0.26
	Al_2O_3		-	-	0.004		0.03	-	0.006		0.21	0.05	0.26
	TiO_2		0.02	0.06	-		0.02	-	-		0.04	0.06	0.007
	Cr_2O_3		0.03	0.02	0.016		0.02	0.08	0.017		0.04	0.05	0.005
	FeO		0.17	0.06	0.06		0.10	0.16	0.08		0.05	0.04	0.025
	MnO		0.04	0.02	0.01		0.03	0.06	0.025		0.01	0.04	0.007
	MgO		0.10	0.09	0.16		0.15	0.06	0.16		0.01	0.03	0.008
	CaO		0.02	-	0.006		0.03	0.02	0.008		0.26	0.03	0.18
	Na_2O		0.02	-			0.02	-	-		0.13	0.03	0.10
	K_2O		0.007	-			0.01	-	-		-	0.04	0.007
	NiO		-	-	0.010		-	0.24	0.016		-	0.09	0.013

present. Even if scientifically meaningless, a negative value should be allowed when an element is not present, as multiple bremsstrahlung-corrected measurements will naturally yield either slightly positive or slightly negative values with an average centred on zero, as is the case with WDS analysis.

In summary, for the same standard-based acquisition conditions including counting time and beam current, WDS results are sometime almost an order of magnitude better in terms of analytical uncertainty (precision) compared to EDS results, especially for minor elements. In terms of accuracy for major and minor elements, equally good standard-based quantitative data can be obtained by WDS or EDS in common silicate minerals.

7. COMBINING EDS-WDS FOR THE BEST OF BOTH WORLDS

Two real-case applications of combined EDS-WDS are presented next. First, an example of minor to trace element analysis (10 - 1,000 ppm range) in apatite with Ca and P analysed by EDS, and second, an example of trace content of P (±Cr and Al) by WDS with a low detection limit of ~ 10 ppm or better in olivine with all major elements by EDS.

7.1. Halogen and trace elements in apatite

Apatite $Ca_5(PO_4)_3(OH,F,Cl)$ is a common phosphate found as an accessory mineral in many different sedimentary, metamorphic, and magmatic rocks. The hydroxyl crystallographic site can be partially to completely replaced by fluorine or chlorine anion. The Ca^{2+} cation can be partially replaced by divalent cation such as Sr, Fe, Mn, or Mg, by trivalent lanthanide especially light rare earth elements, or by Na^{+}. The P^{5+} cation can be substituted for S^{6+} or Si^{4+} (among others). As it grows under different conditions, its composition can potentially be used as a tracer of magmatic and hydrothermal processes [33-35]. Moreover, it is a resistant mineral that can be used for provenance study in sediments [36].

One of our research interests is to gain a better understanding of the life, death, and possible reactivation of volcanic systems, of the growth of magmatic reservoirs, and to evaluate the risk of effusive versus explosive behaviour. To do so, we need to understand the evolution of the volatiles that are key to these processes. Pristine apatite crystals preserved as inclusions in magmatic phenocrysts are excellent candidates to trace the evolution of volatiles, as the phenocryst isolates the apatite and prevents later re-equilibration with the melt. The analytical challenge is primarily their small size, commonly around or below 20 µm. These apatite inclusions have potentially recorded the conditions at the time of the growth of their silicate host mineral, which itself may correspond to a different stage within the ascent and evolution of the magma across the lithosphere. The following part focuses on the analytical setup developed and on the test we performed to ensure accurate analysis. For more geological implications, refer to [34, 35].

Microanalytical work on apatite is challenging as this mineral is well known to suffer from halogens migration and beam damage, and a single apatite crystal might behave differently under the electron beam depending on its crystallographic orientation [37, 38]. It is, therefore, important to assess the electron beam conditions to minimise the beam damage. Several time dependent intensity tests were performed at different beam currents and beam sizes in apatite grains of random orientation, and most apatite appears to support a dose of 10 nA for ~ 2 minutes at a beam size of 3 to 8 µm (maximum recommended with 20 nm carbon coating : 40 nA·s/µm^2; [39]). A 3 µm beam size was only necessary for inclusions smaller than 5 µm.

Analysis of the major elements Ca and P is done by EDS to shorten the analysis time and improve accuracy. The sensitivity of WDS is reserved for halogen elements, with F on LDE1 and Cl on PET-H, along with up to 7 additional cations that are of interest to the researcher. We focussed on Na, Mg, Si, S, Mn, Fe, and Ce (or Nd) as they can potentially be markers of magmatic differentiation. There is a higher risk for damage in apatite at 3 µm compared to 8 µm at 10 nA beam current, yet we monitored the change in intensity using a time dependent intensity correction on the key elements of interest to each study, in our case: F, Cl, S, Ce, and a choice between Mg, Na, and Si. The time dependent intensity correction is also monitored on the F- and Cl-apatite primary standards to correct for the minor migration effect of F and Cl observed in a few grains over the considered analytical conditions. The MAN background correction is used to correct for the bremsstrahlung on all WDS measurements, helping to further maximise the on-peak counting time. The analytical setup is summarised in Table 3.

Table 3. Analytical setup on the JEOL-8230 at ETH Zürich for combined EDS-WDS apatite analysis.

Acc. voltage 15 keV
Beam current 20 nA (standard), 2 to 10 nA (apatite)
Beam size 10 µm (standard), 3 to 8 µm (apatite inclusions)
EDS 30 s live time, T4 time constant (3.2 µs), open window

						2021	*2024*	*2021*	*2024*
Element	**Xtal**	**SP**	**Standard**	**E range [keV]**		**Time [s]**		**Det. limit [ppm]**	
P Kα	EDS	0	Cl-apatite	1.88	2.26	30	30	551	651
Ca Kα	EDS	0	Cl-apatite	3.52	4.18	30	30	487	588
F Kα	LDE1	1	Wilberforce Ap.	*n.a.*		90	80	252	259
Mg Kα	TAP	2	Forsterite	*n.a.*		50	20	66	98
Na Kα	TAP	2	Albite	*n.a.*		10	20	223	159
Si Kα	TAP	2	Albite	*n.a.*		10	20	139	102
S Kα	PETH	3	Anhydrite	*n.a.*		90	80	31	37
Ce Lα	LiFH	4	CePO4	*n.a.*		60	30	300	448
Fe Kα	LiFH	4	Fayalite	*n.a.*		20	30	231	189
Cl Kα	PETH	5	Cl-apatite	*n.a.*		90	80	59	66

This setup is tested against a series of secondary reference materials, notably Durango apatite (NMNH 104021; [30]), and a pair of synthetic F-Cl and F-OH apatite from D. Harlov (APS-17 [F-Cl] from [40] and APS-69 [F-OH] from [41]). Results are shown in Table 4.

Table 4. Average and standard deviation of several analyses in secondary standards APS-17, APS-69, and Durango apatite. Element data in italic and blue were obtained using EDS data, whereas data in black were processed using WDS data. H_2O calculated by stoichiometry. Data in parenthesis represents the 1σ standard deviation from the average; for instance, 41.87(24) is equal to 41.87 ± 0.24.

Method	Pts	Date acq	CaO	P_2O_5	F	Cl	O=F,Cl	H_2O	TOTAL
APS-17	*Reference >*		**54.88**	**41.67**	**2.08**	**2.82**	**-1.51**	***(0.06)***	**100.00**
EDS	*44*	*12.08.20*	*55.31(23)*	*41.87(24)*	*< 0.59*	*3.13(15)*	*-0.71*	*0.98*	*99.75*
WDS	44	12.08.20	55.10(19)	42.19(35)	1.87(9)	3.21(12)	-1.51	0.08	100.89
WDS +*EDS*	11	24.04.24	*54.94(22)*	*41.70(10)*	1.79(9)	3.11(4)	-1.46	0.12	100.10
APS-69	*Reference >*		**55.72**	**42.31**	**1.77**	**-**	**-0.75**	**0.95**	**100.00**
EDS	*68*	*12.08.20*	*55.94(20)*	*42.39(21)*	*0.6(8)*	*< 0.06*	*-0.29*	*1.48*	*98.88*
WDS	68	12.08.20	55.89(17)	42.61(35)	2.65(48)	< 0.007	-1.11	0.55	100.08
WDS +*EDS*	11	24.04.24	*55.84(22)*	*42.30(28)*	3.02(11)	< 0.007	-1.27	0.36	99.91
Durango	*Reference >*		**54.02**	**40.78**	**3.53**	**0.41**	**-1.58**	**-**	**98.18**
EDS	*9*	*12.08.20*	*54.12(13)*	*40.82(16)*	*3.3(6)*	*0.42(6)*	*-1.50*	*0.06*	*98.27*
EDS	*10*	*12.08.20*	*54.22(28)*	*40.91(26)*	*2.4(4)*	*0.39(6)*	*-1.11*	*0.50*	*98.33*
EDS	*10*	*12.08.20*	*54.25(16)*	*41.03(21)*	*3.5(8)*	*0.40(5)*	*-1.55*	*0.01*	*98.66*
WDS	9	12.08.20	54.13(15)	41.02(24)	3.30(10)	0.451(18)	-1.49	0.08	98.63
WDS	10	12.08.20	54.40(19)	41.1(5)	3.22(14)	0.415(17)	-1.45	0.13	98.86
WDS	10	12.08.20	54.27(18)	40.7(4)	3.28(27)	0.429(12)	-1.48	0.09	98.25
WDS +*EDS*	9	24.04.24	*54.26(21)*	*40.82(14)*	3.23(10)	0.391(10)	-1.45	0.13	98.29

Method	# pts	Date acq	SO_3	SiO_2	MgO	FeO	MnO	Na_2O
APS-17	*Reference >*		**-**	**-**	**-**	**-**	**-**	**-**
EDS	*44*	*12.08.20*	*< 0.13*	*0.15(10)*	*< 0.08*	*< 0.17*	*< 0.16*	*< 0.08*
WDS	44	12.08.20	< 0.016	0.036(13)	< 0.017	< 0.021	< 0.020	< 0.020
WDS +*EDS*	11	24.04.24	< 0.009	< 0.022	< 0.016	< 0.024	-	< 0.022
APS-69	*Reference >*		**-**	**-**	**-**	**-**	**-**	**-**
EDS	*68*	*12.08.20*	*< 0.13*	*0.17(7)*	*< 0.08*	*< 0.17*	*< 0.16*	*< 0.08*
WDS	68	12.08.20	< 0.016	0.039(16)	< 0.017	< 0.021	< 0.020	< 0.020
WDS +*EDS*	11	24.04.24	< 0.009	< 0.022	< 0.016	< 0.024	-	< 0.022
Durango	*Reference >*		**0.37**	**0.34**	**0.01**	**0.06**	**0.01**	**0.23**
EDS	*9*	*12.08.20*	*< 0.13*	*0.44(8)*	*0.12(11)*	*< 0.17*	*< 0.16*	*0.30(10)*
EDS	*10*	*12.08.20*	*< 0.13*	*0.42(9)*	*0.13(11)*	*< 0.17*	*< 0.16*	*0.26(6)*
EDS	*10*	*12.08.20*	*< 0.13*	*0.46(8)*	*0.11(6)*	*< 0.17*	*< 0.16*	*0.35(6)*
WDS	9	12.08.20	0.40(3)	0.353(12)	0.024(12)	0.049(10)	0.026(9)	0.287(25)
WDS	10	12.08.20	0.367(20)	0.322(17)	0.025(9)	0.048(10)	0.028(14)	0.251(23)
WDS	10	12.08.20	0.313(14)	0.333(17)	0.027(10)	0.047(12)	0.025(14)	0.256(18)
WDS +*EDS*	9	24.04.24	0.391(15)	0.313(18)	0.025(9)	0.042(10)	-	0.251(18)

Comparison of CaO and P_2O_5 wt% data obtained by EDS or WDS reveals essentially the same results even within a 1σ uncertainty (Fig. 4a; Table 4). Minor elements (< 1 wt%) and light elements (e.g., F) suffer from larger uncertainties with EDS (Fig. 4b; Table 4) and are commonly near or below the detection limit, not detected (e.g., SO_3 in Durango apatite systematically

reported as zero), or slightly overestimated (e.g., SiO_2 in Durango apatite). They can remain accurate for medium to high energy X-rays that suffer little to no interference, with (for instance) excellent results on Cl-Kα at 2.62 keV with 0.39 ± 0.06 to 0.42 ± 0.06 by EDS for a reference value at 0.41 wt%. However, it should be stressed that several points in a homogeneous domain must be acquired, and only the average of those points might approach an accurate data. For lighter elements in low abundance, such as Na and F, the EDS performance is relatively poor and the data should be taken as a rough approximation, especially when individual points are compared. WDS yields distinctly lower uncertainty on F-Kα measurements compared to EDS (Fig. 4b). If we consider all 29 single-point analyses of F in 3 grains of Durango apatite, WDS yields results between 2.83 and 3.72 wt% F with a precise average at 3.27 ± 0.18, whereas EDS yields highly variable results between 1.6 to 4.7 wt% (average 3.06 ± 0.76).

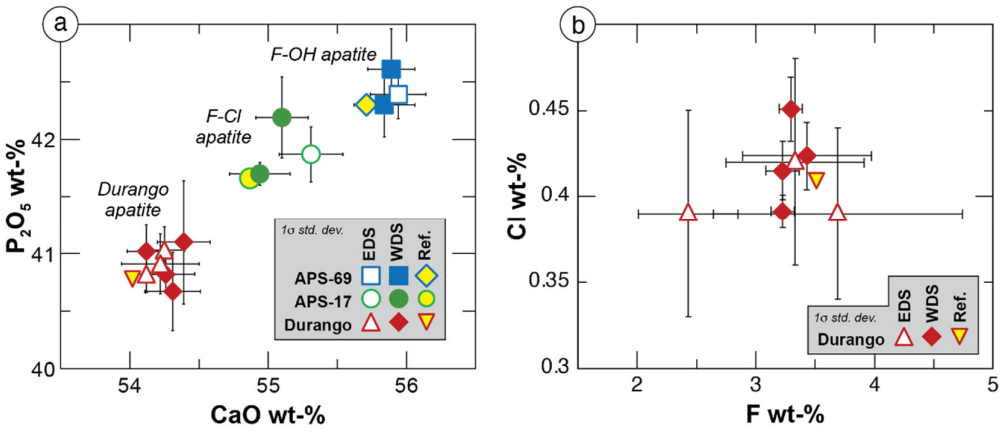

Figure 4. Comparison of analysis by EDS and by WDS of a) major oxide CaO and P_2O_5 in three secondary standards, and b) of halogens F and Cl in Durango apatite. Ref. = reference values from [30, 40, 41].

In terms of accuracy, Fig. 5 shows that WDS results of all measured minor to trace elements are close to the reference values of [30], and to some LA-ICP-MS analyses of Durango apatite performed at ETH Zürich (M. Guillong, pers. comm., 2025). For instance, the 29 WDS analyses yield accurate and precise values at 0.330 ± 0.015 SiO_2 (reference: 0.34 %) and 0.26 ± 0.03 Na_2O (reference: 0.23 %), whereas EDS data varies from ~ 0.3 to 0.6 wt% for SiO_2 and ~ 0.1 to 0.45 wt% for Na_2O. MgO and FeO are expected to yield ~ 0.01 and 0.055 wt%, respectively, which are the values returned by WDS, whereas individual EDS data suggest inaccurate values between 0.1 and 0.4 wt%. In this situation WDS is strongly preferred as it yields precise and accurate results.

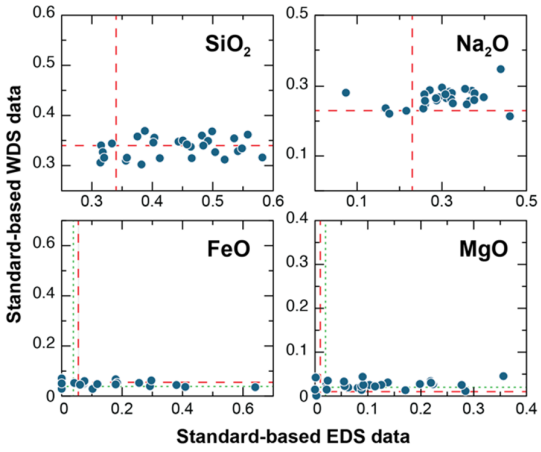

Figure 5. Minor to trace element in Durango apatite analysed by EDS or by WDS given as wt%. Same scale for EDS and WDS is used on each plot. Red dashed line is the reference value of [30]. Green dotted line on FeO and MgO plots are average LA-ICP-MS analyses by M. Guillong (pers. comm., 2025).

7.2. P-in-olivine and other trace elements

Olivine $(Fe,Mg)_2SiO_4$ is a common mantle-related mineral that is typically found in igneous rocks. It can grow through a large range of pressures and temperatures, from the deep asthenosphere up to Earth's surface. To better understand the evolution of mafic magma from its generation in the mantle to its differentiation in the crust, it is common to rely on geochemistry of major, minor, and trace elements which can be easily acquired on EPMA. Divalent cations such as Fe^{2+} and Mg^{2+}, along with others (e.g., Mn^{2+} and Ni^{2+}) have the tendency to rapidly diffuse, thus resetting any history they may have recorded [42]. On the contrary, higher valency cations have a higher probability to retain an original signature, especially phosphorous, as their diffusion is much slower [43, 44]. Phosphorous, an incompatible element in basaltic melts [45], is incorporated into the olivine lattice by the process of growth entrapment during episodes of undercooling, which induces rapid olivine growth [43, 46]. Phosphorous concentrations are proportional to the growth rates [47], with early P-rich skeletal growth containing up to ~ 0.3 wt%, followed by younger crystal with less P. As a result, P-in-olivine acts as a sturdy tracer of the evolution of the mafic magma that was responsible for the formation of the continental and oceanic lithosphere. Besides Earth volcanic samples, our group also studies meteorites, notably a collection of Martian meteorites. As this material is precious, non-destructive techniques such as EPMA are preferred. The example briefly presented here is from an olivine-phyric shergottite, the meteorite Northwest Africa 1110 (NWA1110; [48]).

Getting down to the 1 - 10 ppm level with WDS analysis by EPMA is possible and usually requires a high beam current (≥ 200 nA), long counting time (≥ 2 min), careful background correction, and the aggregation of multiple WDS [21]. The danger of WDS analysis of major elements at these conditions is the saturation of the WDS detector. With a normalised count rate

of up to ~ 650 and 550 cps/nA for Si-Kα on TAP and Mg-Kα on TAP-H in San Carlos olivine respectively, it is expected to receive > 100,000 cps at > 200 nA for those elements. At this rate, the WDS deadtime correction commonly fails. A solution is to rely on the use of EDS to quantify the major elements (Si, Mg, Fe, Mn), and to use all five WDS to analyse only P-Kα or additional elements such as Cr-Kα and Al-Kα (Table 5). For the bremsstrahlung correction, we apply a MAN background correction. This approach can be used accurately for trace elements in simple matrix, providing a blank correction is applied [24, 26]. The X-ray energy region of P-Kα on PET at ~197.4 mm on JEOL (~0.705 sinθ on Cameca) is clear of any major X-ray interference in olivine, offers a high peak-to-background ratio with low bremsstrahlung, and most standards used for the MAN background correction are essentially P-free, guaranteeing a precise bremsstrahlung correction. To further ensure accuracy, a blank correction was applied using a synthetic pure forsterite standard, yet it was almost always unnecessary and overachieving the correction as the uncertainty on each measurement was bigger than this correction. This blank correction varied slightly from session to session but essentially remained within ± 10 to 20 ppm. For instance, a series of 10-point analyses in Springwater, San Carlos, and a synthetic forsterite in one session yielded respectively 6 ± 3, 11 ± 3, and -1 ± 2 ppm, with a detection limit around 8 ppm. The virtually P-free synthetic forsterite serves as an excellent blank-correction standard, and its value can hardly be better to prove that we can accurately measure the absence of an element, a requirement for trace element analysis [49]. It should be noted for the EDS community that this assessment can only be properly done if negative values are considered and not defaulted to zero.

Table 5. Analytical setup on the JEOL-8230 at ETH Zürich for combined EDS-WDS olivine analysis, either for P or for Al and Cr.

Acc. voltage 15 keV
Beam current 20 nA (std), 200 nA (olivine)
Beam size 10 µm (std), 0 µm (olivine)
EDS 3.2 or 1.6 µs (55 or 35 DT%), reduced window

							*40 s**	*60 s**	*120 s**
Element	**Xtal**	**SP**	**Standard**	**E range [keV]**		**Time [s]**	**Det. limit [ppm]**		
Si Kα	EDS	0	Forsterite	1.60	2.01	30	302	291	303
Mg Kα	EDS	0	Forsterite	1.06	1.43	30	287	271	281
Mn Kα	EDS	0	Pyrolusite	5.68	6.70	30	516	514	460
Fe Kα	EDS	0	Fayalite	6.18	7.28	30	690	657	481
P Kα	PET	1	Wilberforce Ap.	*n.a.*		40-120*	29	23	17
P Kα	PET	2	Wilberforce Ap.	*n.a.*		40-120*	31	25	18
P Kα	PET-L	3	Wilberforce Ap.	*n.a.*		40-120*	16	13	9
P Kα	PET-H	4	Wilberforce Ap.	*n.a.*		40-120*	14	12	8
P Kα	PETH	5	Wilberforce Ap.	*n.a.*		40-120*	20	16	11
All P Kα, aggregated			**Wilberforce Ap.**	***n.a.***		**200-600**	**9**	**8**	**5**

* P Kα analysed for 40, 60, or 120 s on peak on each spectrometer.

Alternative WDS setup for Al and Cr in olivine

Element	**Xtal**	**SP**	**Standard**	**E range [keV]**	**Time [s]**	**D.L.**
Al Kα	TAP	1	Anorthite	*n.a.*	120	10
Al Kα	TAP	2	Anorthite	*n.a.*	120	10
Cr Kα	PET-L	3	Chromite	*n.a.*	120	11
Cr Kα	PET-H	4	Chromite	*n.a.*	120	17
Al Kα	TAPH	5	Anorthite	*n.a.*	120	19
All Al aggregated			**Anorthite**	***n.a.***	**360**	**8**
All Cr aggregated			**Chromite**	***n.a.***	**240**	**9**

For the study of the Martian meteorites, first we map the sample qualitatively using EDS on our SEM to locate the olivine grains of interest based on their preserved Fe-Mg zoning, and selected olivine grains are checked for their orientation using EBSD (not shown here). Three to four grains in each sample are selected for quantitative element mapping by WDS to reveal zoning of major elements and trace elements such as P. It should be noted here that quantitative combined EDS-WDS mapping exists, notably with PROBE FOR EPMA software, yet it is not compatible with the EDS hardware we currently have. Combined EDS-WDS quantitative mapping with the JEOL software would require a minimum of 1 to 2 additional passes for the acquisition of the bremsstrahlung intensity. For the time being, we rely on a two-pass stage mapping technique: A quick map at 20 to 100 nA of the major elements (Fig. 6), followed by a second map of the same area only for P-Kα on five spectrometers at high current (500 or 1,000 nA; Fig. 7). Alternatively, a single high-current map of P on five WDS can be accurately quantified, given that a fixed composition for all major elements representative of the analysed olivine grain is specified and the mapped olivine does not show too strong zoning notably in Fe and Mg. This is necessary to guarantee accurate matrix and MAN background corrections. Map quantification is done using CALCIMAGE following [50], and an example is given in Fig. 7.

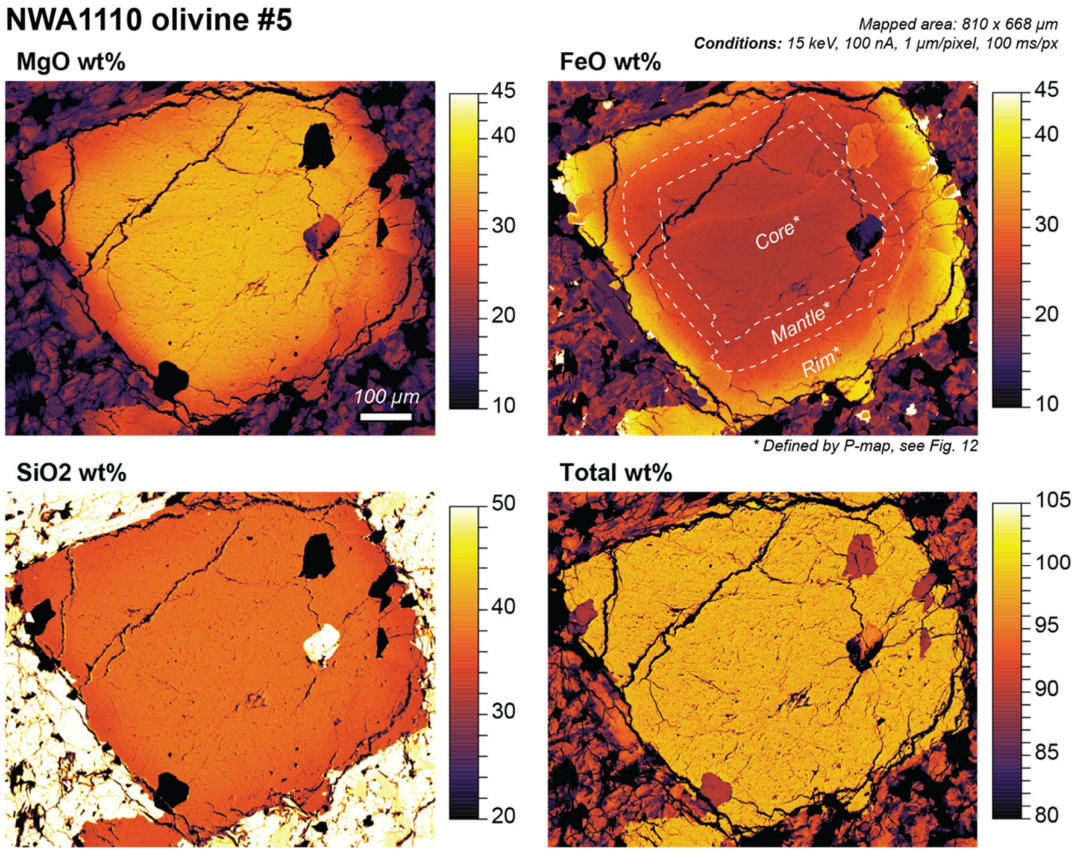

Figure 6. Quantitative element map of major element (Si, Fe, and Mg) in olivine 5 of NWA1110.

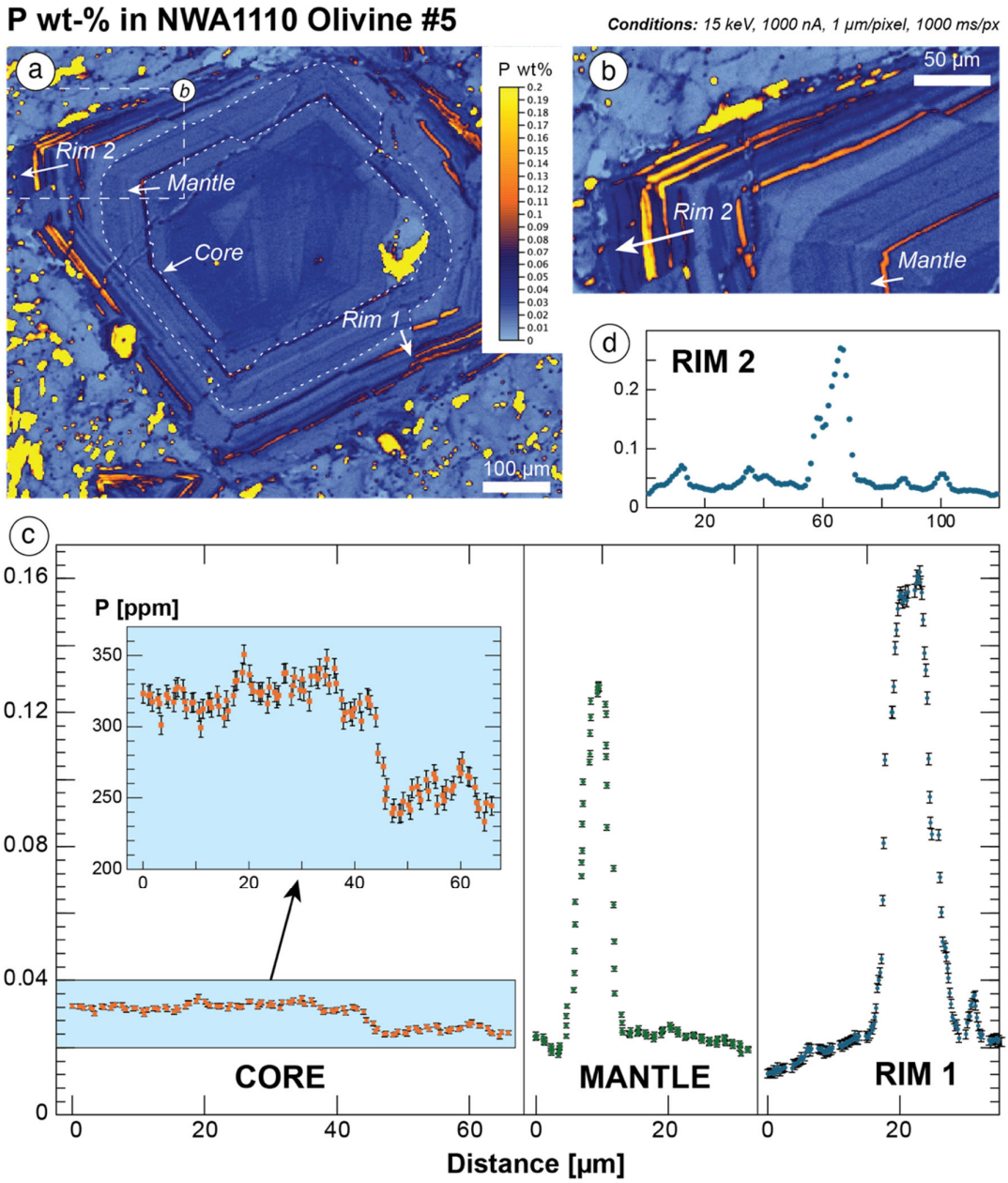

Figure 7. Quantitative element map of P obtained by WDS and P analyses in wt% through several line in NWA1110 meteorite, olivine #5 (Arka et al., in prep.). Uncertainty is at 2σ level. The line traverses are oversampled with a step size of 0.3 to 0.5 µm, while the analysed X-rays are emitted from a diameter ~ 800 nm around the electron beam, and the electron beam is most likely around 1 µm at the considered beam energy and current.

In addition to element maps, detailed point analyses were obtained along selected transects. Whereas Fe and Mg maps only show a late diffusional profile at the grain rim (if any), P-zoning in olivine grains from several Martian meteorites commonly highlights different zones that can be classified as "core", "mantle", and "rim" (highlighted on the FeO map in Fig. 6). For instance,

several olivine grains in NWA1110 show a P-poor core with some preserved skeletal and dendritic H-shaped zoning in the centre core (not visible in Fig. 7), with a P-poor outer core around 200 ppm, followed by a mantle with a distinct sharp P band yielding ~ 1,000 ppm, and ending with a series of oscillatory P-rich and P-poor bands at the corner of the grains and a clear increase in the maximum P-content between mantle and rim, which can yield 1,500 to 3,000 ppm (e.g., rims 1 and 2; Fig. 7). This initial growth is interrupted and followed by an episode of high undercooling, which induces another rapid overgrowth of the mantle zone of the olivine. Prior to the rim growth, resorption of the olivine is indicated by the discontinuity in the subtle oscillatory zoning near the mantle edge. This resorption could have been caused by the mixing with a hotter magma. The rapid oscillatory P-rich rims again suggest a rapid growth with high undercooling. Overall, this combined EDS-WDS study permits a better understanding of undercooling induced growth during magma ascent in the Martian crust. Additional details on this geological, or rather areological, study will hopefully be available soon in [51].

8. CONCLUSIONS AND OUTLOOK

This paper proves once and for all that precision and accuracy of EDS data for major and minor elements acquired on Si-drift detectors can be as accurate and precise as WDS analysis, notably in many geological materials (silicates, phosphates, etc.), providing that (a) a standard-based approach using the *k*-ratio is considered, (b) an adequate matrix correction is used, (c) the working distance is set to the optimum of the EDS detector (proper take-off angle and geometry in general), (d) beam current, time constant, and ultimately DT% are appropriately set, and (e) no strong X-ray interference exists. The analysis of beam sensitive material such as alkali-rich hydrous glass requires a lower current and shorter analysis time, ideally over a large area whenever possible. In this situation, the X-ray collection efficiency of large area SDD can outperform WDS detectors for major and some minor elements, even with WDS equipped with a large area monochromator or H-type spectrometer.

If possible, EDS data should always be acquired with WDS analysis. Even if the analyst prefers quantitative analyses by WDS, EDS data may still be used (a) as a safeguard for quantification of some elements if something went wrong with a WDS, (b) to understand why some analytical totals are unexpectedly low or high (i.e., misidentification of the expected phase), or (c) for quantifying a minor to major "surprise element" such as Ba in K-feldspar. For this latter case, an EDS standardisation could be done the day after, and the data could be re-processed after the analysis, which is not the case with WDS as the element to be analysed must be defined beforehand. EDS standardisation appears to be stable over several months. Providing the instrument and environment conditions remain stable, a daily standardisation of EDS may not be necessary. However, it does not take more time to systematically acquire EDS during the acquisition of each standard.

EDS quantitative analysis generally fails at providing reliable trace element data below ~ 1.0 to 0.5 wt%, and this is where WDS detector is necessary for precise and accurate microanalytical work. Accurate data can sometimes be obtained by averaging multiple short EDS analyses of ~ 30 s, yet the data will still suffer from a higher uncertainty compared to WDS, along with possible false identification of elements not present (or present in much lower content). Although not discussed here, EDS can potentially fail at providing reliable and precise data when the analysed X-ray peak severely overlaps with another element. Accurate data can potentially be obtained, but with a large uncertainty and possible inaccuracies.

Standard-based quantitative EDS analysis should be viewed as a complimentary detector to WDS for quantitative analysis on EPMA or SEM. Quantification of interference-free major elements should be considered by EDS, and minor and trace elements or elements that require a higher sensitivity by WDS. This contribution describes two successful applications with combined EDS-WDS analysis at low and at high current of trace elements in apatite and in olivine, respectively. EDS and WDS element maps can also be combined and quantified, but such a discussion would require another paper.

EDS and WDS are just two detectors among many others that can detect and measure photons! The more recent development of soft X-ray emission spectrometry (SXES) has set a precedent on spectral energy resolution for low X-ray energy (50 to 2,000 eV) with peak-to-background benchmarks that should still be evaluated, and certainly a lot of hidden information on the shape and energy level of each X-ray transition that can potentially tell us more about the valence and coordination state of an ion [52-55]. SXES reaches ~ 0.2 eV resolution at the Al-L emission and can see very low X-ray energies, reaching down to the Li-K line around 50 eV [56, 57]. The future is certainly in the combination of not only EDS and WDS as discussed here, but also SXES and any other useful signals to the researcher that can be collected simultaneously, notably cathodoluminescence spectra. For this, it would be necessary that companies selling EDS and WDS hardware (and other detectors on EPMA or SEM) would allow third party software and individual scientific programmers to take advantage of their hardware and potentially help to develop new capabilities for data treatment and acquisition.

9. ACKNOWLEDGEMENTS

SEM and EPMA work and instruments at ETH Zürich were fully supported by the Department of Earth and Planetary Sciences and ETH Zürich. Support from NSF (USA) is acknowledged for the JEOL-8230 at the University of Colorado Boulder (NSF EAR-1427626). Tim Rose and the Smithsonian Institute (USA) are warmly thanks for providing microbeam analytical standards used in this study, along with Daniel Harlov (GFZ Potsdam, Germany) for providing synthetic apatite.

10. STATEMENT

No artificial intelligence and only human brain power was used throughout the science and writing of this paper.

11. REFERENCES

[1] Newbury D E, Swyt C R and Myklebust R L 1995 *Anal. Chem.* **67** 1866-1871

[2] Castaing R 1951 *Application of electron probes to local chemical and crystallographic analysis*. PhD thesis. [Paris, France: University of Paris]

[3] Bastin G F and Heijligers H J M 1990 *Scanning* **12** 225-236

[4] Armstrong J T 1995 *CITZAF: a package of correction programs for the quantitative electron microbeam X-ray analysis of thick polished materials, thin films and particles*. in: Microbeam Analysis 4 177-200

[5] Pouchou J-L and Pichoir F 1991 *Quantitative Analysis of Homogeneous or Stratified Microvolumes Applying the Model "PAP."* in: Electron probe quantification. (Heinrich K F J and Newbury D E; Eds.) [New York, NY: Plenum Press] 31-75

[6] Fitzgerald R, Keil K and Heinrich K F J 1968 *Science* **159** 528-530

[7] Gatti E and Rehak P 1984 *Nucl. Instr. Methods Phys. Res.* **225** 608-612

[8] Lechner P, Eckbauer S, Hartmann R, et al. 1996 *Nucl. Instrum. Methods Phys. Res. A* **377** 346-351

[9] Newbury D E and Ritchie N W M 2019 *Microsc. Microanal.* **25** 1075-1105

[10] Newbury D E and Ritchie N W M 2015 *J. Mater. Sci.* **50** 493-518

[11] Newbury D and Ritchie N 2009 *Microsc. Microanal.* **15** 6-7

[12] Newbury D, Ritchie N, Mengason M and Scott K 2017 *Microsc. Microanal.* **23** 1026-1027

[13] Ritchie N W M, Newbury D E, Lowers H and Mengason M 2018 *IOP Conf. Ser: Mater. Sci. Eng.* **304** 01213

[14] Seddio S M 2018 *How to not do poor standards-based EDS quantitative X-ray microanalysis : A WDS perspective*. in: M&M 2018 - Microscopy and Microanalysis meeting, Pre-meeting congress X61 10-11

[15] Allaz J M, Jercinovic M J and Williams M L 2020 *IOP Conf. Ser. Mater. Sci. Eng.* **891** 012001

[16] Llovet X, Moy A, Pinard P T and Fournelle J H *Prog. Mater. Sci.* **116** 100673

[17] Goldstein J I, Newbury D E, Echlin P, et al. 2003 *Scanning electron microscopy and X-ray microanalysis*. [Boston, MA: Springer US]

[18] Reed S J B 1993 *Electron microprobe analysis, 2nd Edition*. [Cambridge, UK: Cambridge University Press]

[19] Seddio S M 2019 *Microsc. Microanal.* **25** 836-837

[20] Seddio S M and Fournelle J H 2015 *Microsc. Microanal.* **21** 1877-1878

[21] Jercinovic M J, Williams M L, Allaz J and Donovan J J 2012 *IOP Conf. Ser. Mater. Sci. Eng.* **32** 1-22

[22] Batanova V G, Sobolev A V and Kuzmin D V 2015 *Chem. Geol.* **419** 149-157
[23] Allaz J M, Williams M L, Jercinovic M J, et al. 2019 *Microsc. Microanal.* **25** 30-46
[24] Donovan J J, Lowers H A and Rusk B G 2011 *Amer. Mineralogist* **96** 274-282
[25] Fialin M, Rémy H, Richard C and Wagner C 1999 *Amer. Mineralogist* **84** 70-77
[26] Donovan J J, Singer J W and Armstrong J T 2016 *Amer. Mineralogist* **101** 1839-1853
[27] Donovan J J and Tingle T N 1996 *Microsc. Microanal.* **2** 1-7
[28] Matthews M, Moran K, Camus P and Wuhrer R 2025 *Is it time to stop using gas flow proportional counters?* in: Book of Tutorials and Abstracts of the EMAS 2025 - 18th European Workshop on Modern Developments and Applications in Microbeam Analysis. [Zürich, Switzerland: EMAS]
[29] Jarosewich E 2002 *J. Res. Nat. Inst. Stand. Technol.* **107** 681
[30] Jarosewich E, Nelen J A and Norberg J A 1980 *Geostand. Newslett.* **4** 43-47
[31] Liu Y, Yang W, Zhang C, et al. 2023 *Geostand. Geoanal. Res.* **47** 595-608
[32] McAleer R J, Aleinikoff J N, Walsh G J and Powell N E 2023 *Electron microprobe analyses of feldspars and petrographic, geochemical, and geochronologic data from the Hawkeye Granite Gneiss and Lyon Mountain Granite Gneiss in the Adirondacks of New York (ver. 2.0, May 2023)*. U.S. Geological Survey, [Reston, VA: U.S. Geological Survey]
[33] Bouzari F, Hart C J R, Bissig T and Barker S 2016 *Econ. Geology* **111** 1397-1410
[34] Popa R-G, Tollan P, Bachmann O, et al. 2021 *Chem. Geol.* **570** 120170
[35] Keller F, Popa R-G, Allaz J, et al. 2023 *Japan. Earth Planet. Sci. Lett.* **622** 118400
[36] O'Sullivan G, Chew D, Kenny G, et al. 2020 *Earth Sci. Rev.* **201** 103044
[37] Stormer J C, Pierson M L and Tacker R C 1993 *Amer. Mineralogist* **78** 641-648
[38] Goloff B, Webster J D and Harlov D E 2012 *Amer. Mineralogist* **97** 1103-1115
[39] Allaz J M, Popa R-G, Reusser E and Martin L 2019 *Microsc. Microanal.* **25** 2312-2313
[40] Schettler G, Gottschalk M and Harlov D E 2011 *Amer. Mineralogist* **96** 138-152
[41] Hughes J M, Harlov D and Rakovan J F 2018 *Amer. Mineralogist* **103** 1981-1987
[42] Chakraborty S 2010 *Rev. Mineral. Geochem.* **72** 603-639
[43] Watson E B, Cherniak D J and Holycross M E 2015 *Amer. Mineralogist* **100** 2053-2065
[44] Nelson W, Hammer J and Shea T 2024 *Geochim. Cosmochim. Acta* **386** 74-83
[45] Toplis M J, Libourel G and Carroll M R 1994 *Geochim. Cosmochim. Acta* **58** 797-810
[46] Milman-Barris M S, Beckett J R, Baker M B, et al. 2008 *Contr. Mineral. Petrol.* **155** 739-765
[47] Welsch B, Faure F, Famin V, et al. 2013 *J. Petrology* **54** 539-574
[48] Russell S S, Zipfel J, Grossman J N and Grady M M 2002 *Meteoritics Planet. Sci.* **37** A157-A184
[49] Jercinovic M, Williams M, Allaz J and Donovan J 2011 *Microsc. Microanal.* **17** 576-577
[50] Donovan J J, Allaz J M, von der Handt A, et al. 2021 *Amer. Mineralogist* **106** 1717-1735
[51] Chatterjee A P, Allaz J, Huber C, et al. 2025 *Phosphorus zoning in olivines: A rosetta stone for tracking magma ascent and storage in the Martian crust*. (in preparation)
[52] Koshiya S and Yokoyama T 2025 *Latest developments of the soft X-ray emission spectrometer and soft X-ray self-absorption structure analysis*. in: Book of Tutorials and Abstract of the EMAS 2025 - 18th European Workshop on Modern Developments and Applications in Microbeam Analysis. [Zürich, Switzerland: EMAS]

[53] Lormand C, Cacciatore E, Gies N B, et al. 2025 *Towards the ferric iron quantification in silicate minerals and glasses: approach using the soft Fe La-Lβ X-ray lines by SXES*. in: Book of Tutorials and Abstracts of the EMAS 2025 - 18th European Workshop on Modern Developments and Applications in Microbeam Analysis. [Zürich, Switzerland: EMAS]
[54] Piccoli F, Dubacq B, Gies N B, et al. 2025 *Iron valence state determined by l-emission spectra: towards a multi mineral calibration?* in: Book of Tutorials and Abstracts of the EMAS 2025 - 18th European Workshop on Modern Developments and Applications in Microbeam Analysis. [Zürich, Switzerland: EMAS]
[55] MacRae C 2025 *Development and application of soft X-ray spectroscopy*. in: Book of Tutorials and Abstracts of the EMAS 2025 - 18th European Workshop on Modern Developments and Applications in Microbeam Analysis. [Zürich, Switzerland: EMAS]
[56] Takahashi H, Murano T, Takakura M, et al. 2016 *IOP Conf. Ser.: Mater. Sci. Eng.* **109** 012017
[57] Yamamoto Y, Morita H, Yamada H, et al. 2016 *Microsc. Microanal.* **22** 640-641